



NARODOWE
CENTRUM
BADAŃ
JĄDROWYCH
ŚWIERK

Filling mass gaps in stellar graveyard by LIGO-Virgo data

Adam Zadrożny

NCBJ Yearly Seminar 2020

Warszawa, 15 December 2020



LIGO
Scientific
Collaboration



Presentation is based on following articles

- GW190521: A Binary Black Hole Merger with a Total Mass of 150 Msun, Phys. Rev. Lett. 125, 101102 (2020)
- Properties and astrophysical implications of the 150 Msun binary black hole merger GW190521, Astrophys. J. Lett. 900, L13 (2020)
- GW190814: Gravitational Waves from the Coalescence of a 23 Solar Mass Black Hole with a 2.6 Solar Mass Compact Object, Astrophys. J. Lett. 896, L44 (2020)
- GW190425: Observation of a compact binary coalescence with total mass ~ 3.4 Msun, Astrophys. J. Lett. 892, L3 (2020)
- GWTC-2: Compact Binary Coalescences Observed by LIGO and Virgo During the First Half of the Third Observing Run, arXiv:2010.14527
- Population properties of compact objects from the second LIGO-Virgo Gravitational-Wave Transient Catalog, arXiv: 2010.14533

Ways to observe universe

- Electromagnetic

- Visible light
- Radio frequencies
- Infra-red
- ...



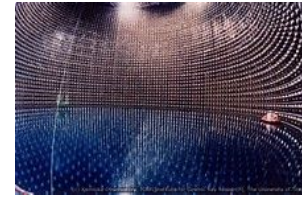
Credit: CAMK



Credit: Pi of the Sky



- Neutrinos ... and cosmic rays



Credit: Super Kamiokande Team



- Gravitational waves (from 2015)



Credit: Virgo



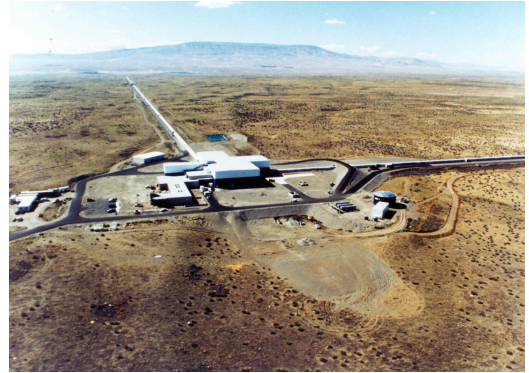
Credit: LIGO

Gravitational Wave Detectors

LIGO Livingston

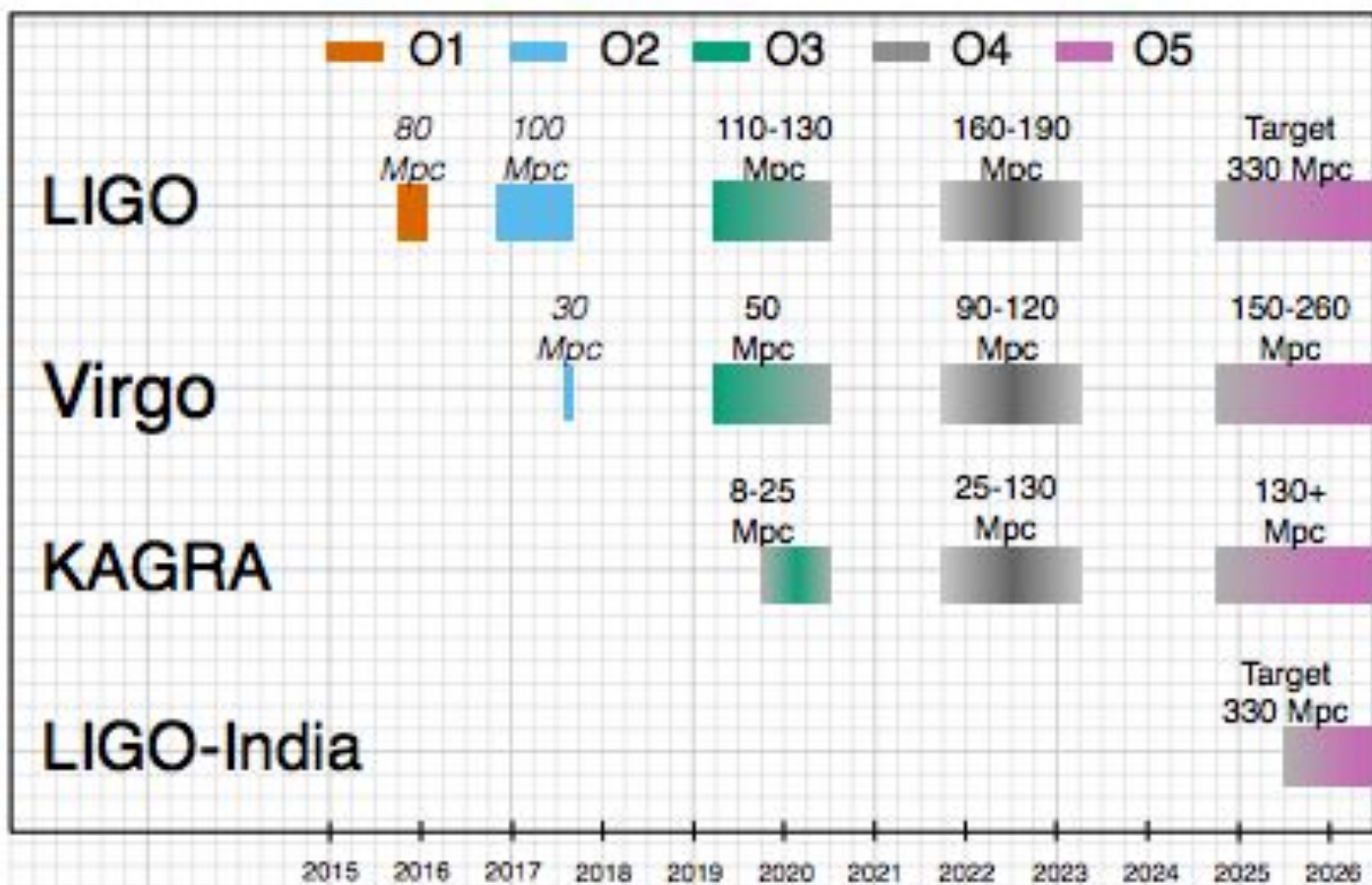


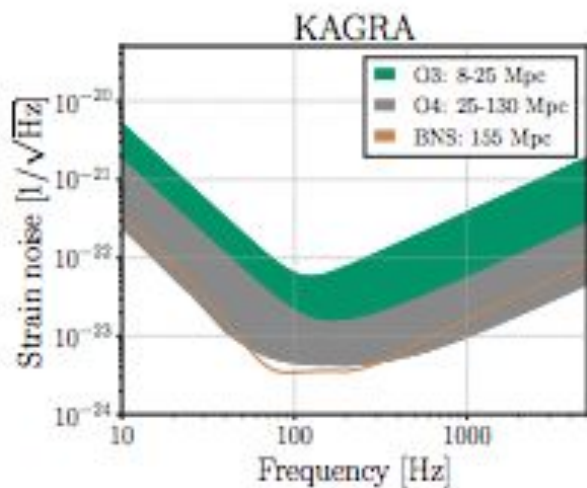
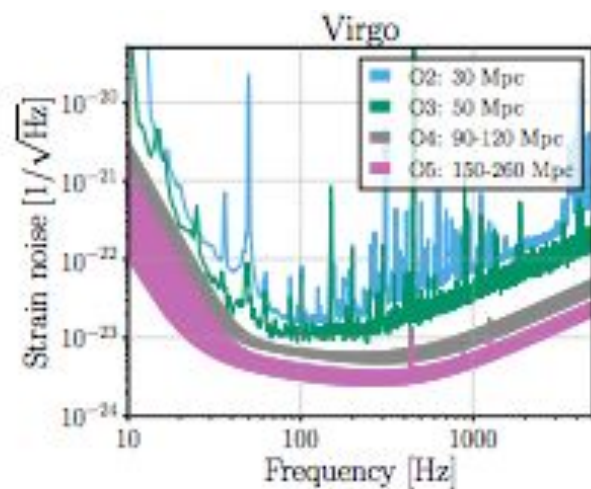
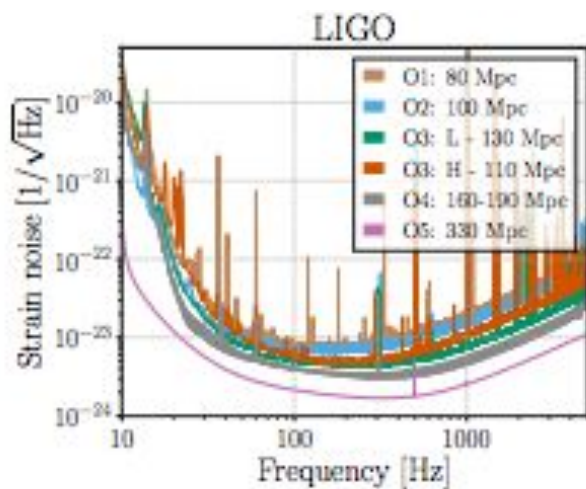
LIGO Hanford



Virgo







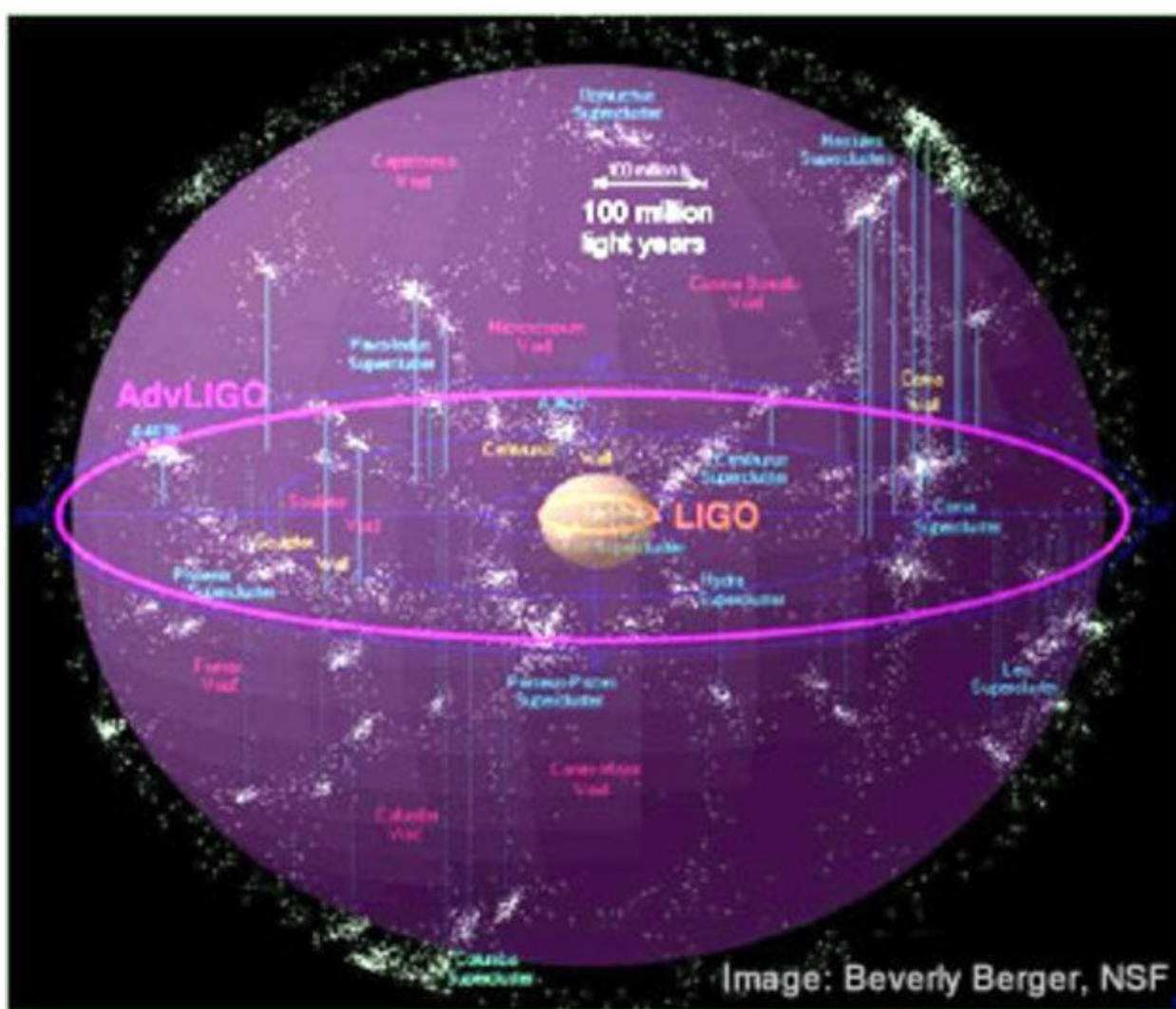
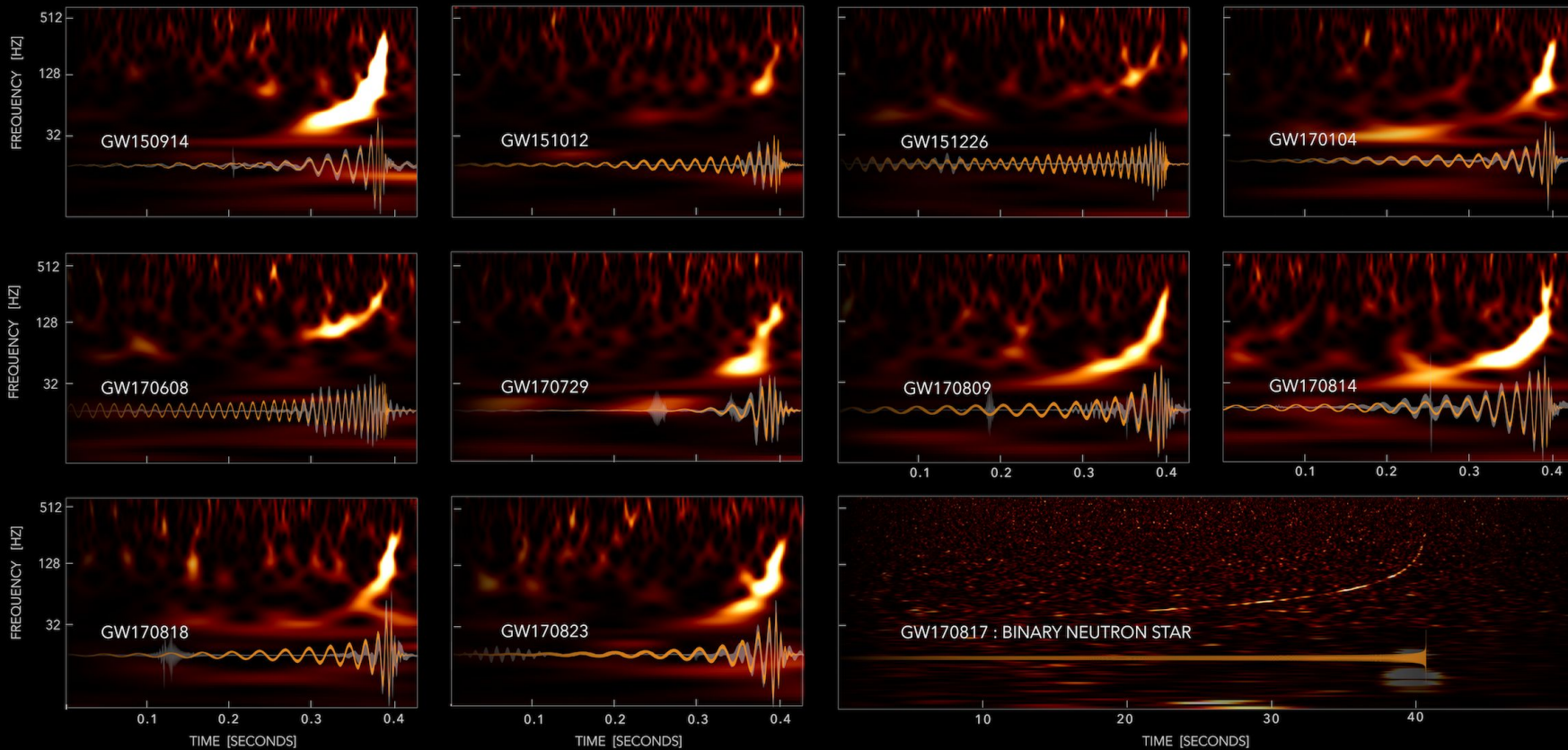


Image: Beverly Berger, NSF

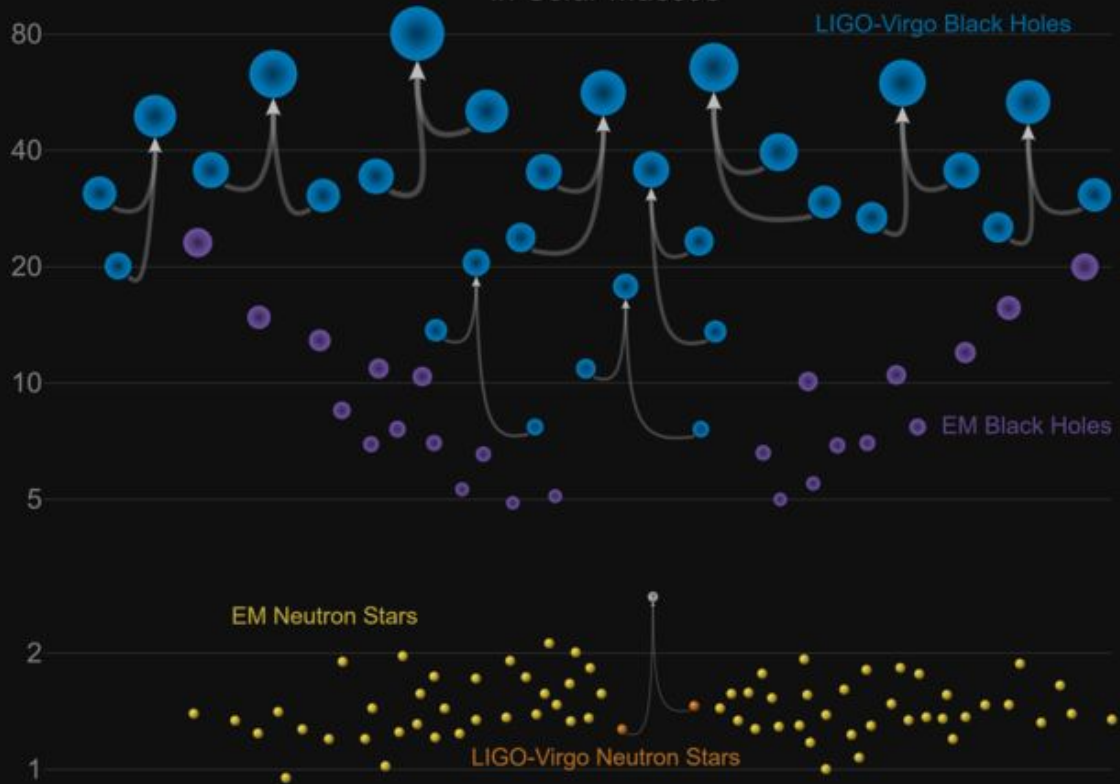
GRAVITATIONAL-WAVE TRANSIENT CATALOG-1



Prior to O3

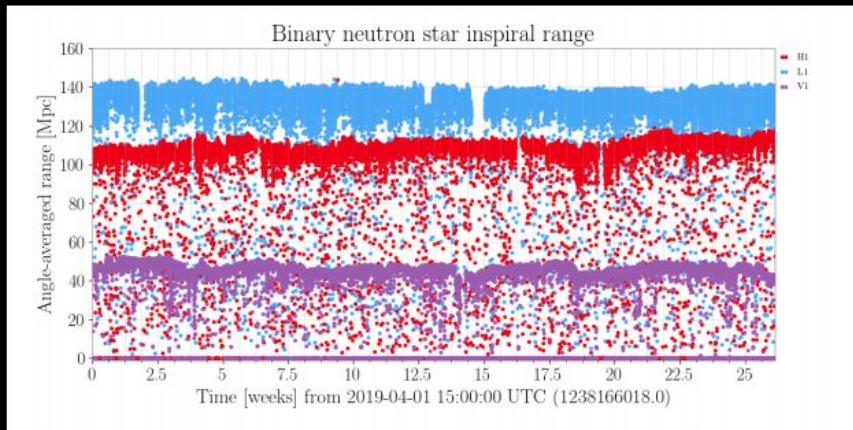
Masses in the Stellar Graveyard

in Solar Masses



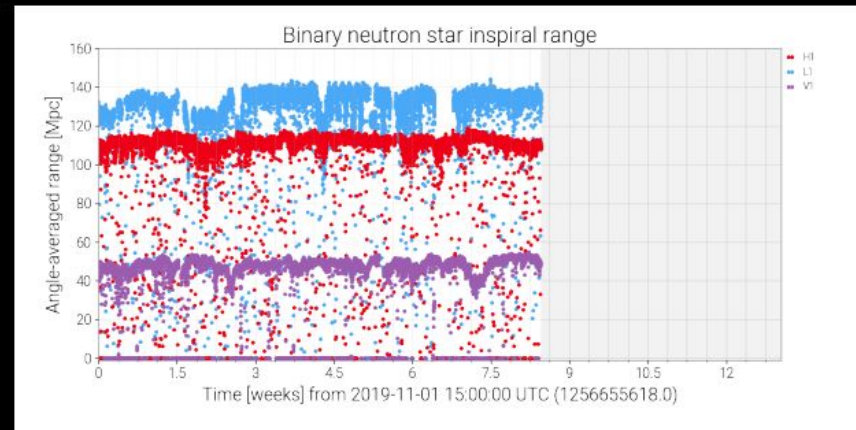
LIGO-Virgo's 3rd Observation Run

O3a



April 1 - October 1, 2019

O3b



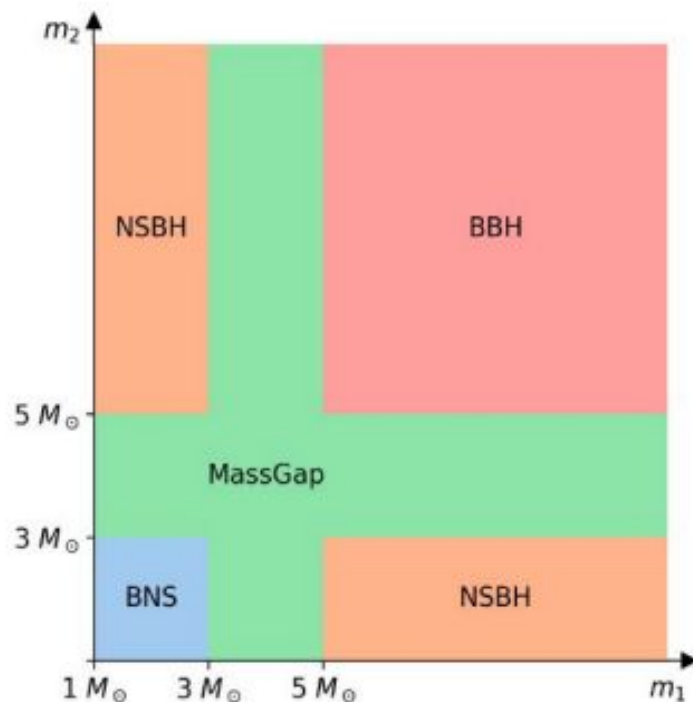
November 1, 2019 - April 2020

3rd observation run (O3)

- The O3 run
 - Start: 1 April 2019
 - Break: Oct 2019
 - End: 30 April 2019
- LIGO/Virgo low-latency public alerts for transient event candidates
 - Notices and circulars available through the Gamma-ray Coordinates Network (GCN)
https://gcn.gsfc.nasa.gov/gcn3_archive.html
- Event candidates will be publicly available
 - <https://gracedb.ligo.org>
- Japanese KAGRA detector to joined in Feb 2020

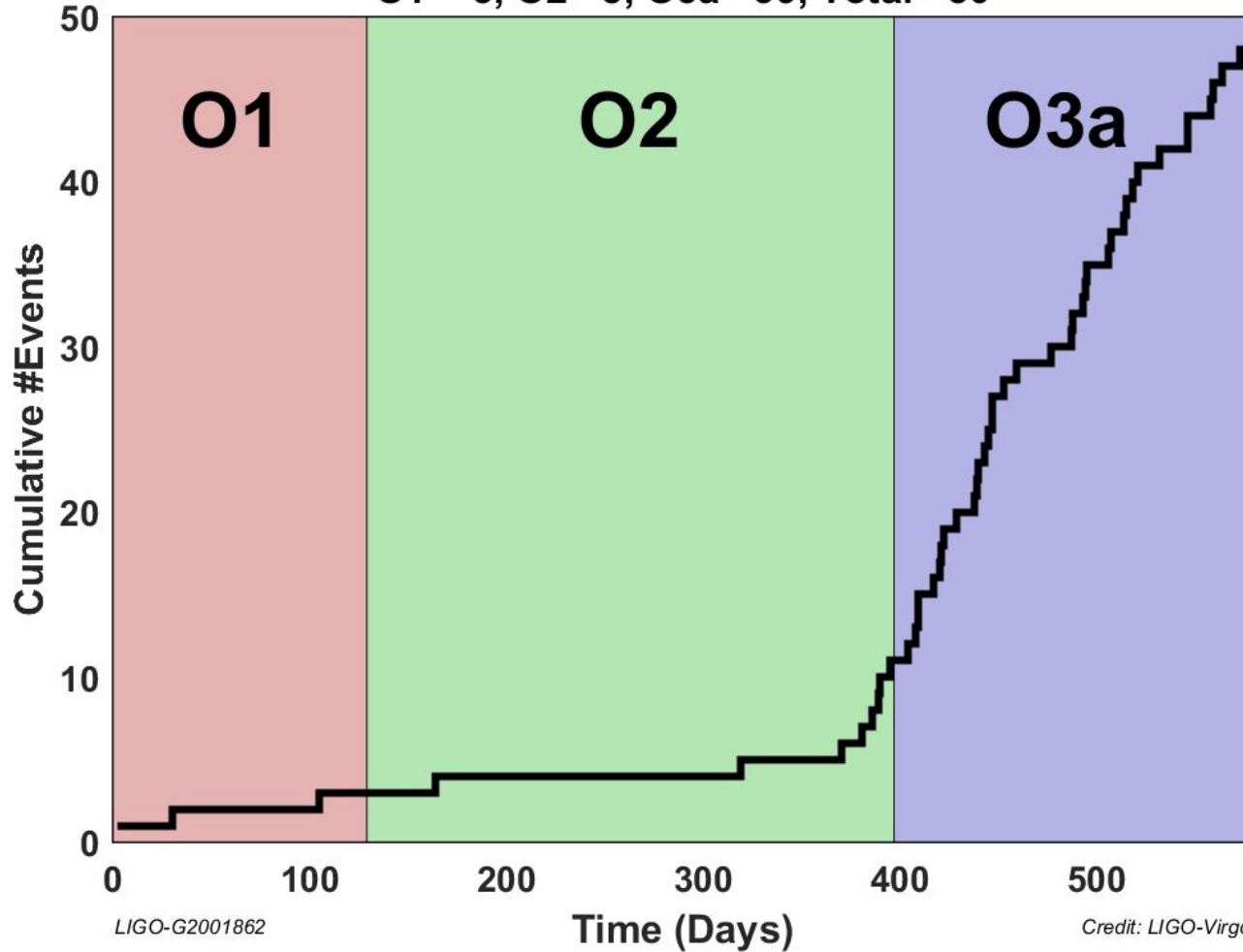
Inference: classification

- Five numbers, summing to unity, giving probability that the source belongs to the following five categories:
 - Terrestrial, BNS, MassGap, NSBH, BBH
 - GW150914: $5e-40$, 0.00, 0.06, 0.01, 0.93
 - GW170817: $1e-48$, 1.00, 0.00, 0.00, 0.00



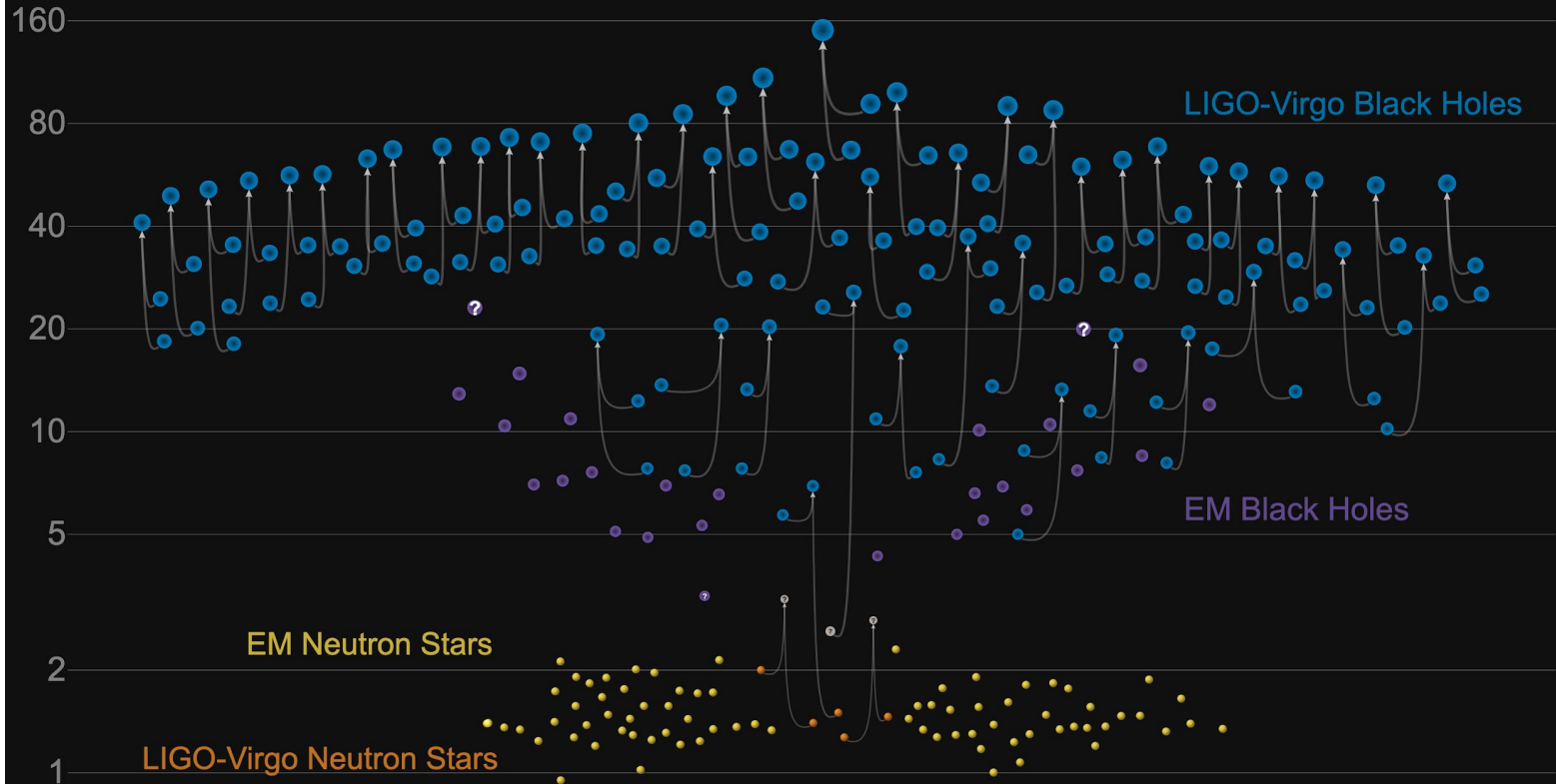
Cumulative Count of Events

O1 = 3, O2 = 8, O3a = 39, Total = 50



Masses in the Stellar Graveyard

in Solar Masses



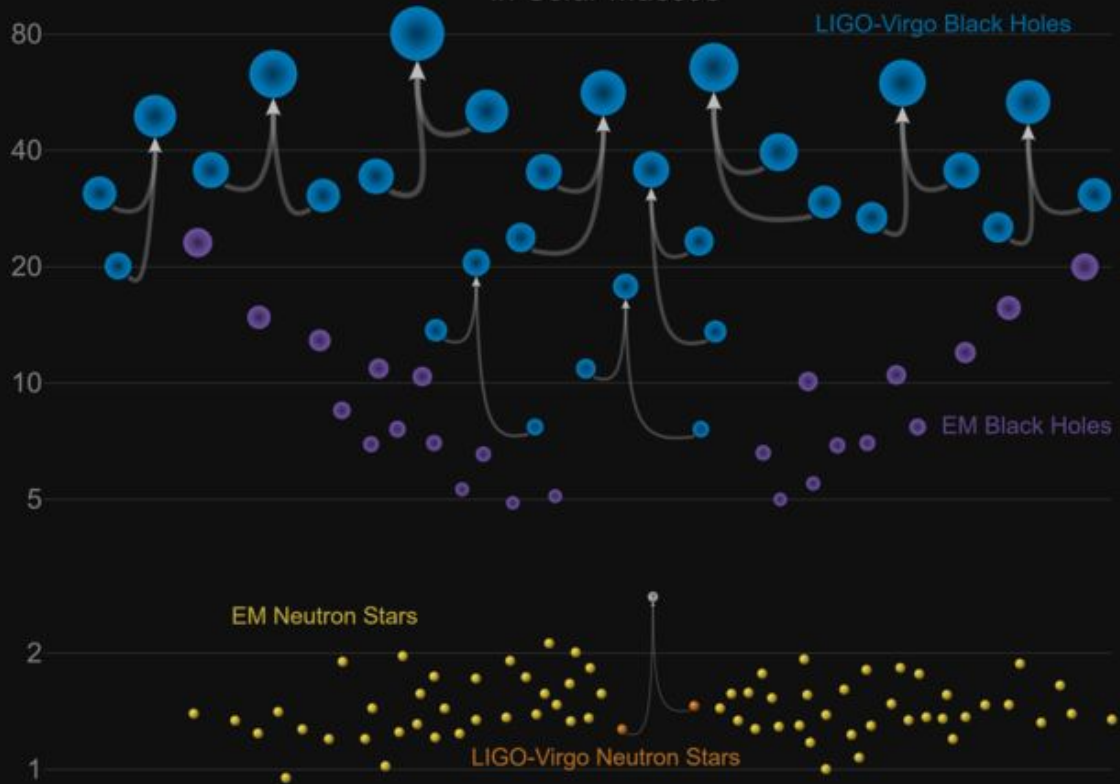
GWTC-2 plot v1.0

LIGO-Virgo | Frank Elavsky, Aaron Geller | Northwestern

Prior to O3

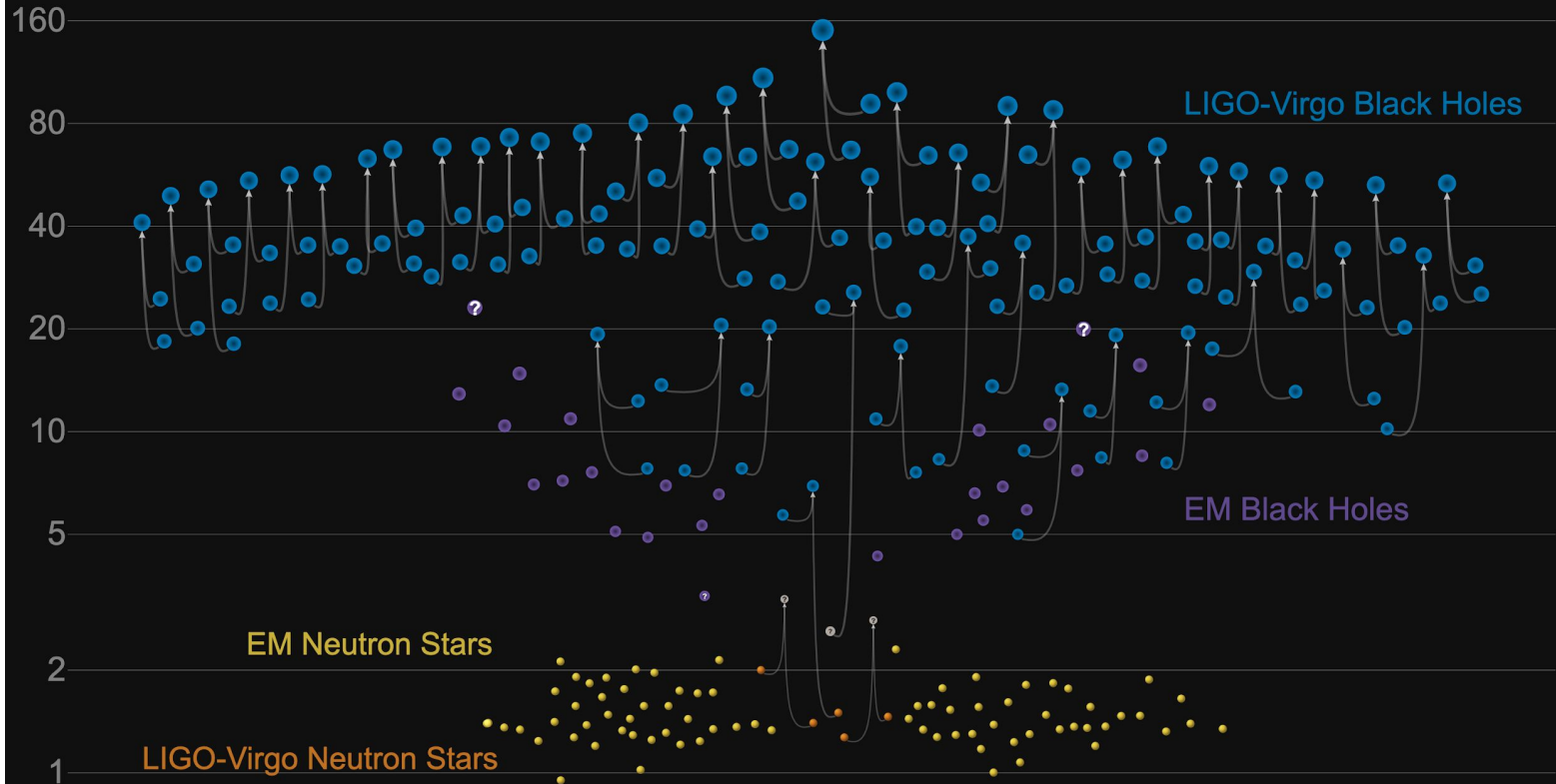
Masses in the Stellar Graveyard

in Solar Masses



Masses in the Stellar Graveyard

in Solar Masses

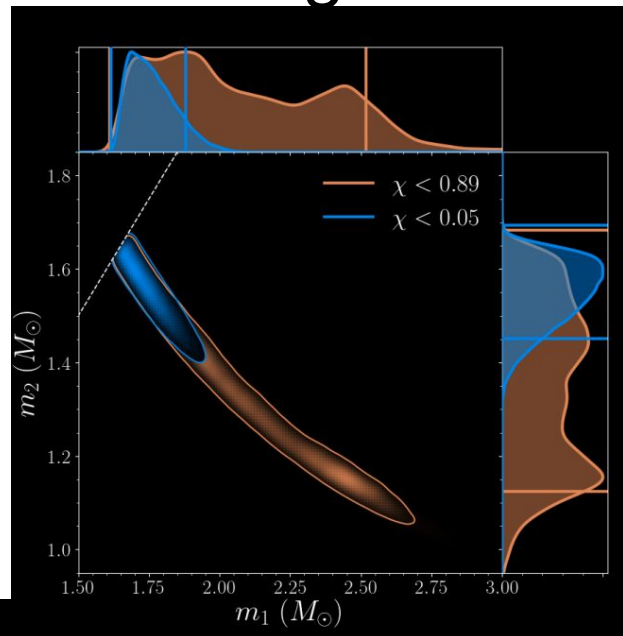


GWTC-2 plot v1.0

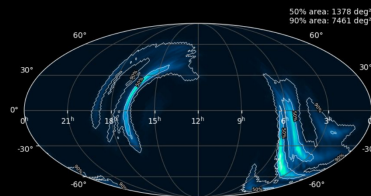
LIGO-Virgo | Frank Elavsky, Aaron Geller | Northwestern

GW190425 - second binary neutron star merger

- Second BNS observed
- Components
 - First: 1.61 - 2.52 M_{sun}
 - Second: 1.12 - 1.68 M_{sun}
 - Total mass: 3.3 - 3.7 M_{sun}
- Result object in massgap region
- Poor localization
- No GRB counterpart
- No matter effects observed

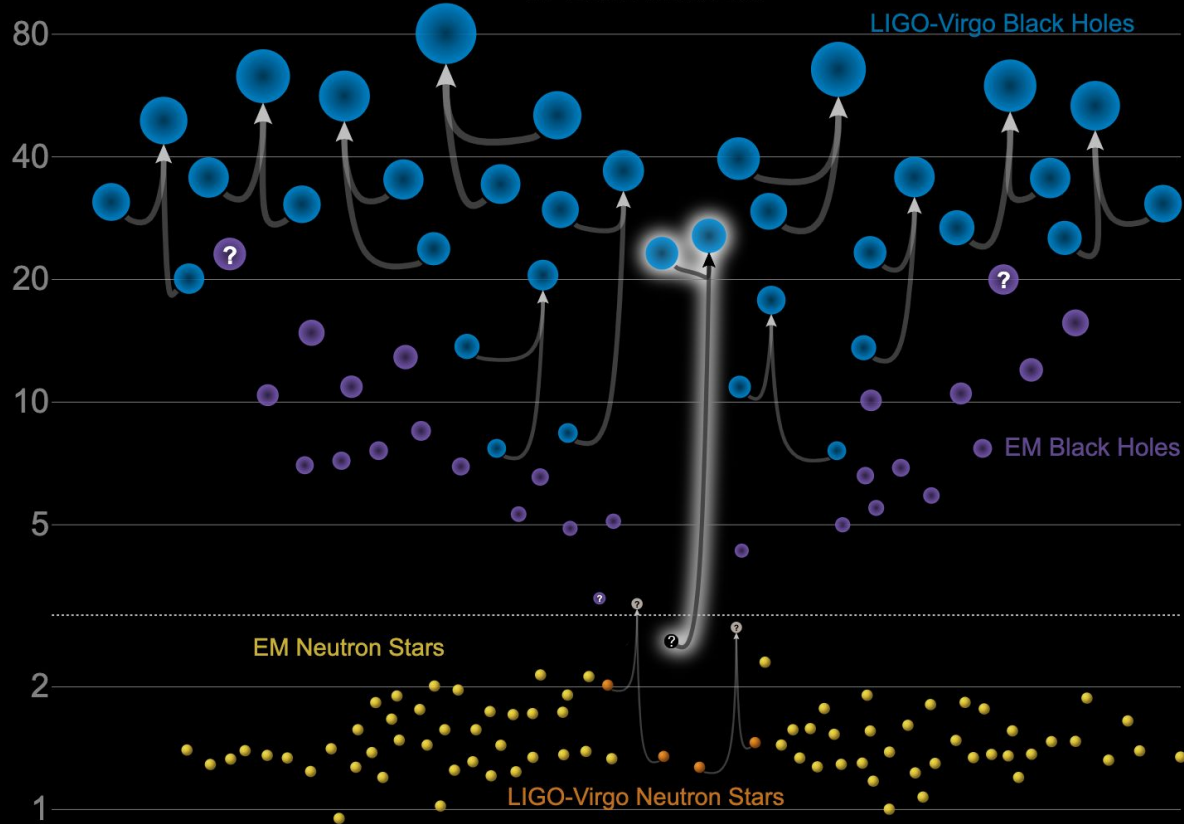


S190425z



Masses in the Stellar Graveyard

in Solar Masses

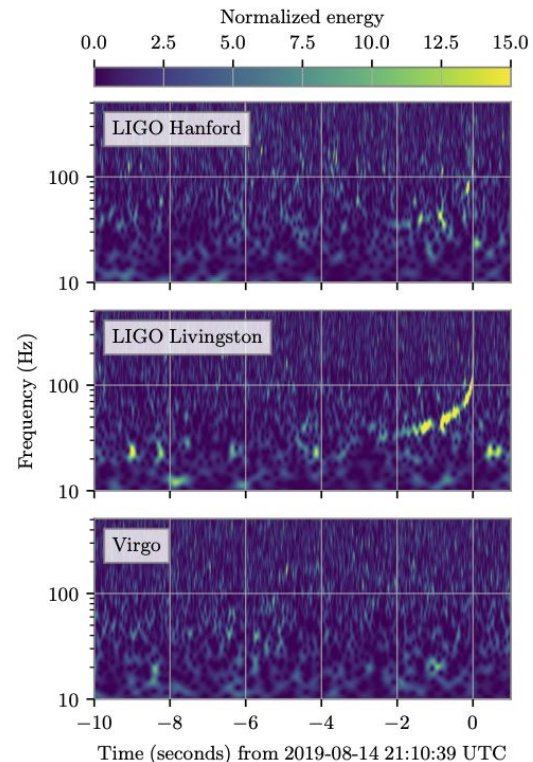


Updated 2020-05-16

LIGO-Virgo | Frank Elavsky, Aaron Geller | Northwestern

GW190814 - gravitational waves from an atypical coalescing binary

- Heavier component has 23 solar masses
- Lighter component has between 2.5 and 3 solar masses
- Mass ratio 1:9
- The lighter component is either
 - an heaviest NS
 - or a lightest BH
- Higher GW modes were observable
- New GR tests were possible



GW190521 - most massive BBH merger up to date

- component masses
 - 66 Msun
 - 85 Msun [!!!]
 - this cannot be a result of a core-collapse due to pair instability
- most massive merger up to date
- first intermediate black hole observed in LIGO 100-1000 Msun mass
- ApJL 900,L13 (2020)

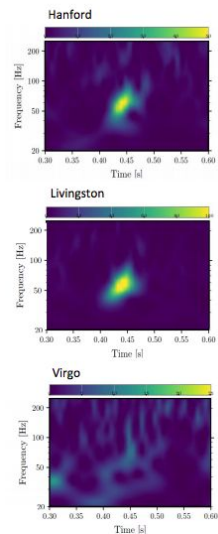
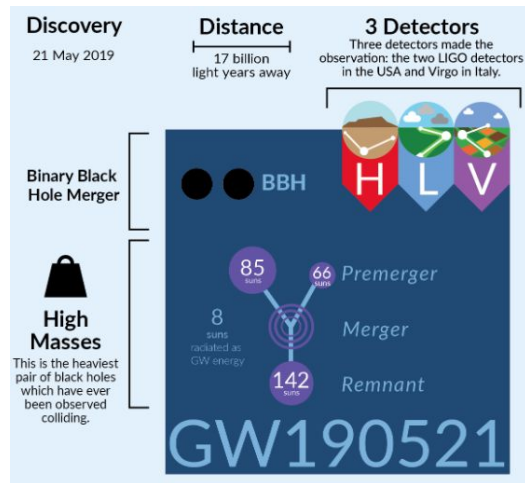
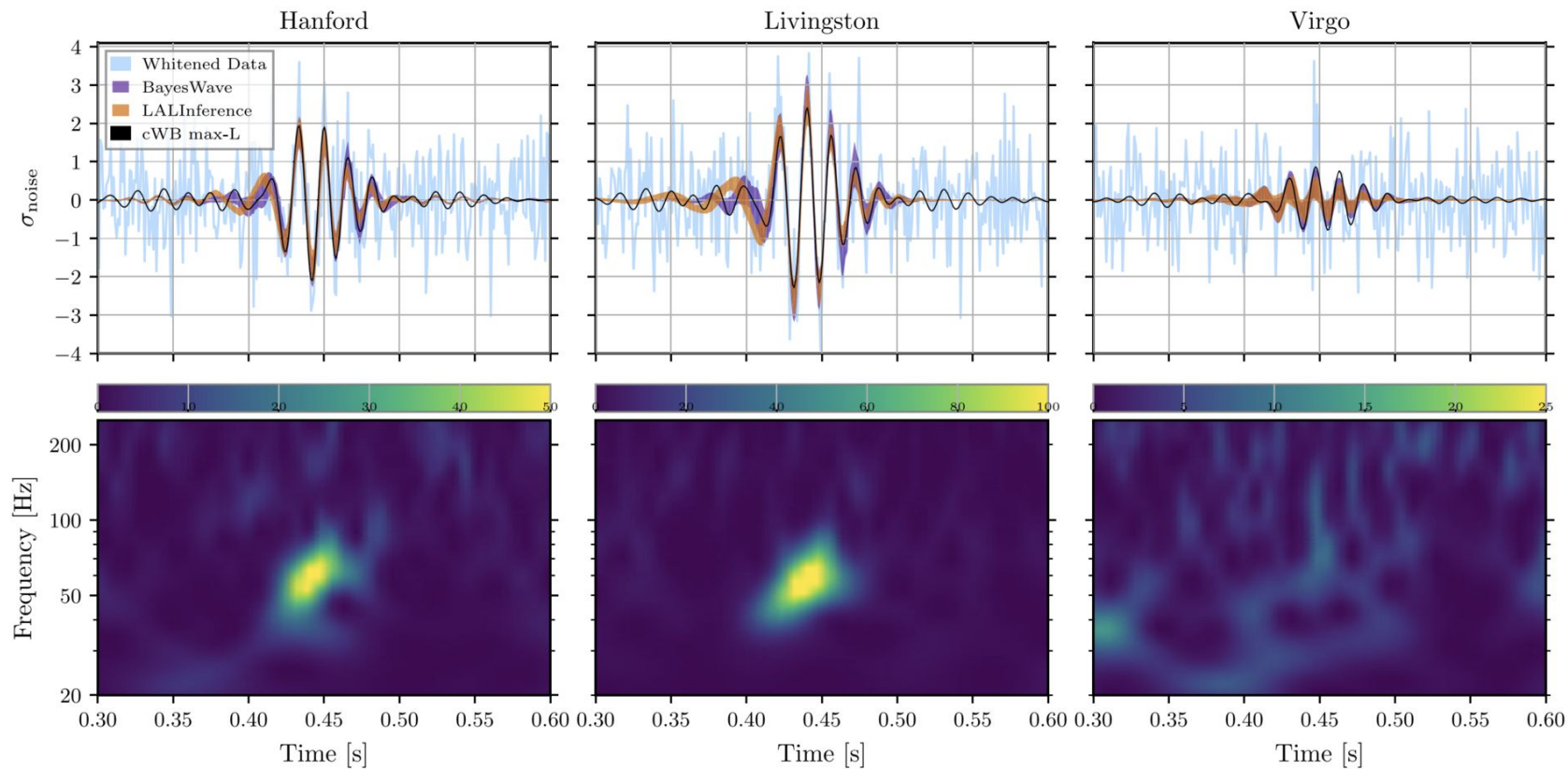


Figure 1. Time-frequency representations of data containing the GW190521 signal, observed by LIGO Hanford (top), LIGO Livingston (middle), and Virgo (bottom). Times are shown relative to 03:02:29 UTC on May 21, 2019. The energy in a certain time-frequency bin is represented by the color palette. Note the signal's extremely short duration and its peak frequency of about 60 Hz. (Adapted from Fig. 1 of our GW190521 discovery paper)

GW190521



GW190521

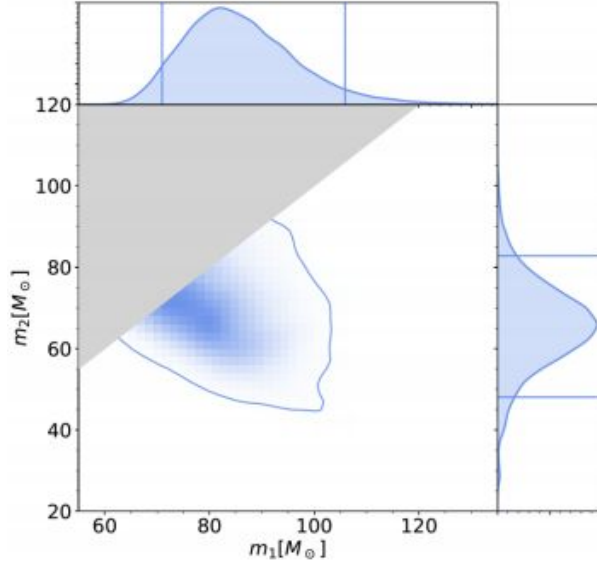
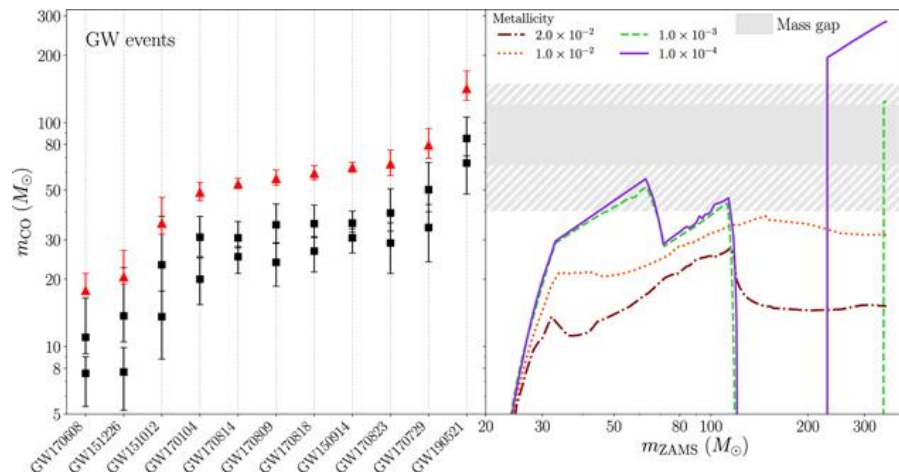
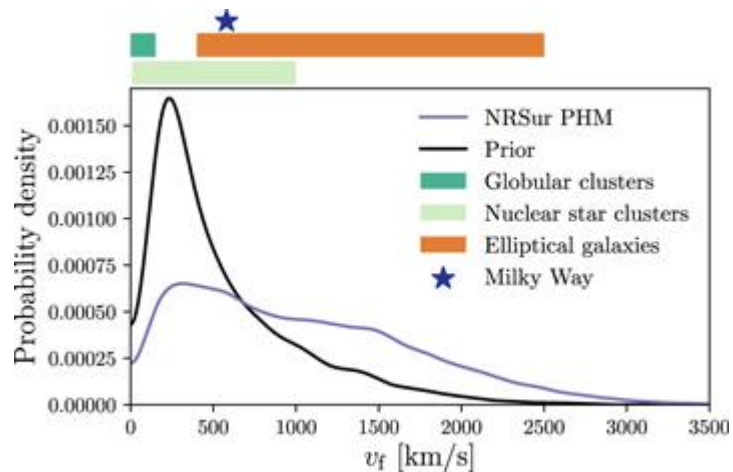


Figure 2. Measured masses of the colliding black holes that produced the gravitational wave signal GW190521 shown as probability distributions. According to the LIGO-Virgo analysis, the true values of the black hole masses have a 90% probability of being located inside the solid blue contour in the central plot (which shows the joint probability for both masses). The same is true for the solid vertical and horizontal lines in the bell-shaped curves to the top and right of the figure, which show the mass measurements for the individual black holes. The grayed-out region of the central plot is due to the LIGO-Virgo convention that the “primary” mass m_1 is always of equal or greater value than the “secondary” mass m_2 . (Reproduced from Fig. 2 of our [GW190521 discovery paper](#))

Table 1
Source Properties for GW190521: Median Values with 90% Credible Intervals That Include Statistical Errors

Waveform Model	NRSur PHM	Phenom PHM	SEOBNR PHM
Primary BH mass $m_1 (M_\odot)$	85^{+21}_{-14}	90^{+23}_{-19}	99^{+42}_{-19}
Secondary BH mass $m_2 (M_\odot)$	66^{+17}_{-18}	65^{+16}_{-18}	71^{+21}_{-28}
Total BBH mass $M (M_\odot)$	150^{+29}_{-17}	154^{+25}_{-16}	170^{+36}_{-23}
Binary chirp mass $\mathcal{M} (M_\odot)$	64^{+13}_{-8}	65^{+11}_{-7}	71^{+15}_{-10}
Mass ratio $q = m_2/m_1$	$0.79^{+0.19}_{-0.29}$	$0.73^{+0.24}_{-0.29}$	$0.74^{+0.23}_{-0.42}$
Primary BH spin χ_1	$0.69^{+0.27}_{-0.62}$	$0.65^{+0.32}_{-0.57}$	$0.80^{+0.18}_{-0.58}$
Secondary BH spin χ_2	$0.73^{+0.24}_{-0.64}$	$0.53^{+0.42}_{-0.48}$	$0.54^{+0.41}_{-0.48}$
Primary BH spin tilt angle θ_{LS1} (deg)	81^{+64}_{-53}	80^{+64}_{-49}	81^{+49}_{-45}
Secondary BH spin tilt angle θ_{LS2} (deg)	85^{+57}_{-35}	87^{+63}_{-58}	93^{+61}_{-60}
Effective inspiral spin parameter χ_{eff}	$0.08^{+0.27}_{-0.36}$	$0.06^{+0.31}_{-0.39}$	$0.06^{+0.34}_{-0.35}$
Effective precession spin parameter χ_p	$0.68^{+0.25}_{-0.37}$	$0.60^{+0.33}_{-0.44}$	$0.74^{+0.21}_{-0.40}$
Remnant BH mass $M_f (M_\odot)$	142^{+28}_{-16}	147^{+23}_{-15}	162^{+25}_{-22}
Remnant BH spin χ_f	$0.72^{+0.09}_{-0.12}$	$0.72^{+0.11}_{-0.15}$	$0.74^{+0.12}_{-0.14}$
Radiated energy $E_{\text{rad}} (M_\odot c^2)$	$7.6^{+2.2}_{-1.9}$	$7.2^{+2.2}_{-2.2}$	$7.8^{+2.8}_{-2.1}$
Peak Luminosity ℓ_{peak} (erg s^{-1})	$3.7^{+0.7}_{-0.9} \times 10^{56}$	$3.5^{+0.7}_{-1.1} \times 10^{56}$	$3.5^{+0.8}_{-1.4} \times 10^{56}$
Luminosity distance D_L (Gpc)	$5.3^{+2.4}_{-2.6}$	$4.6^{+1.6}_{-1.6}$	$4.0^{+2.0}_{-1.8}$
Source redshift z	$0.82^{+0.28}_{-0.34}$	$0.73^{+0.20}_{-0.22}$	$0.64^{+0.25}_{-0.26}$
Sky localization $\Delta\Omega$ (deg^2)	774	862	1069

GW190521



GW190521 - EM candidate S190521g

<https://journals.aps.org/prl/abstract/10.1103/PhysRevLett.124.251102>

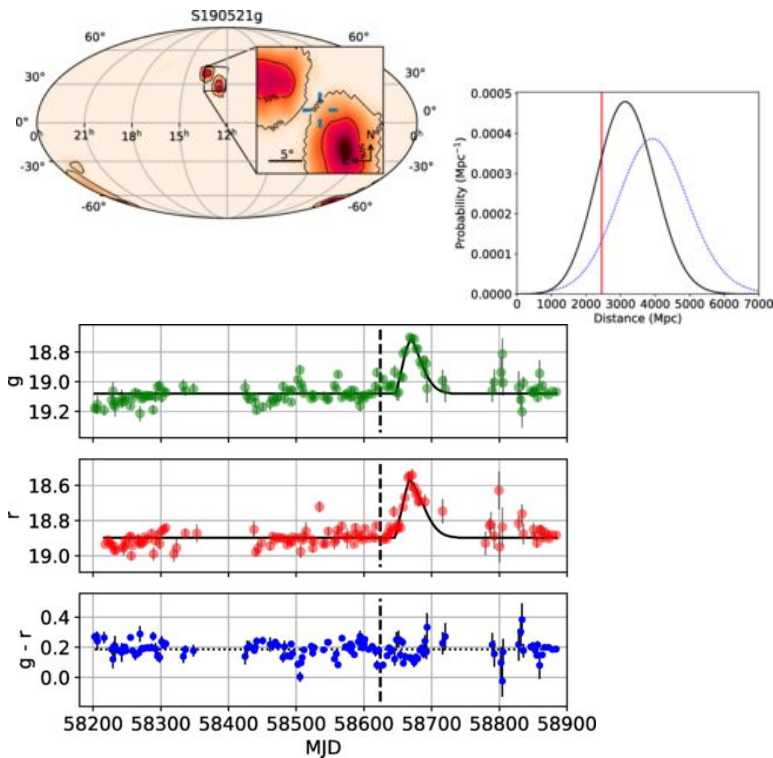
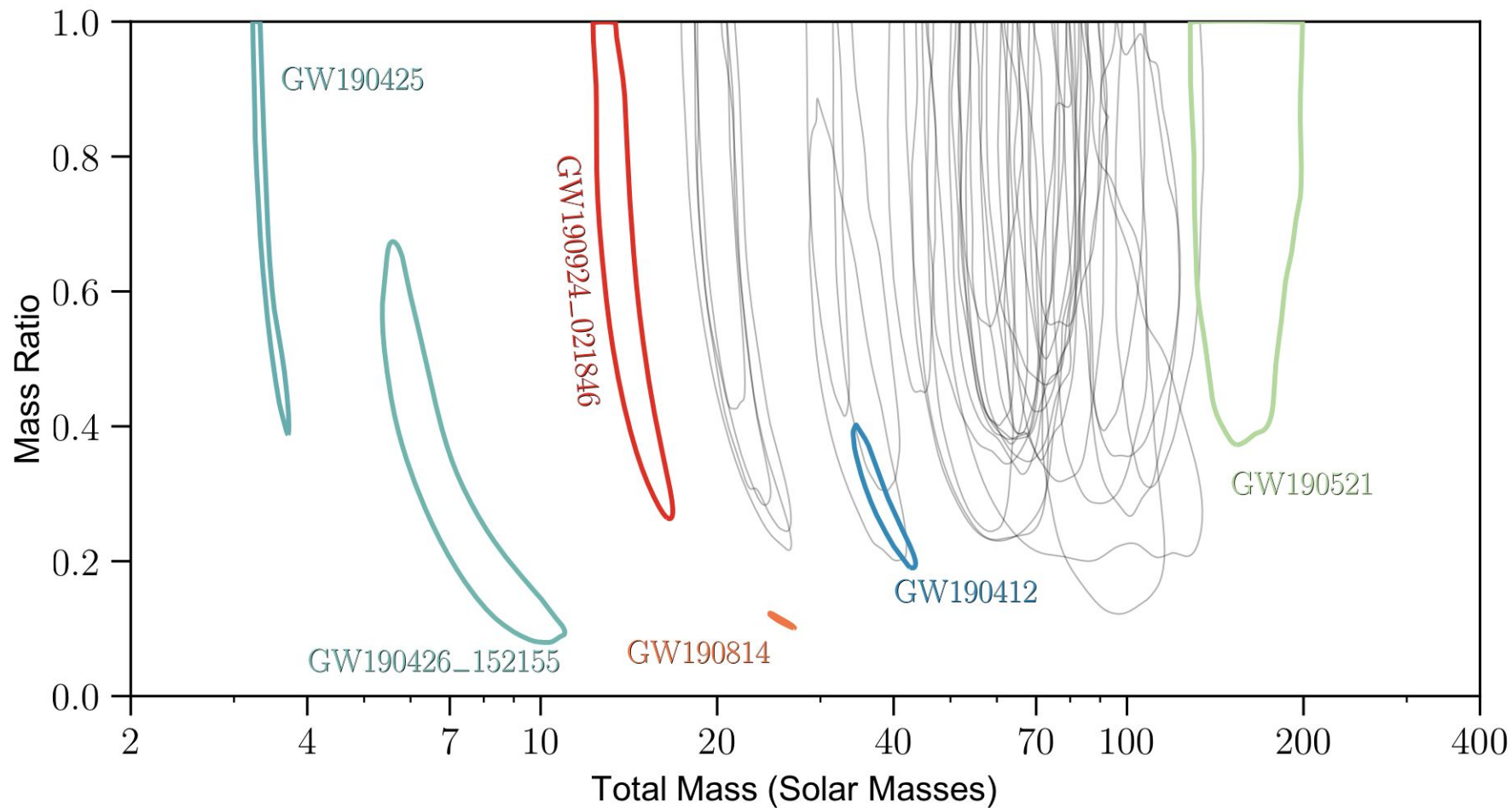
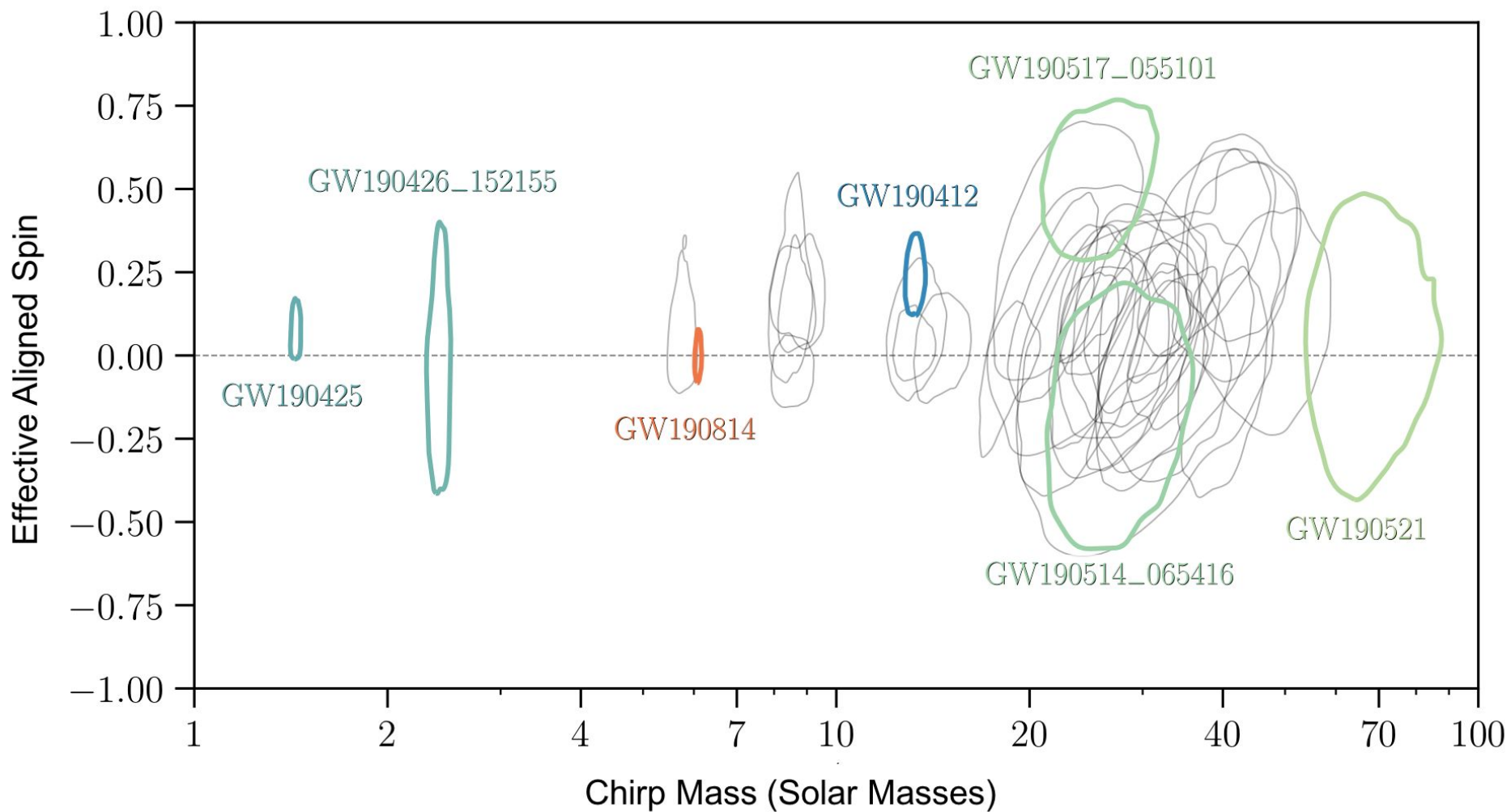


Table 1
Source Properties for GW190521: Median Values with 90% Credible Intervals That Include Statistical Errors

Waveform Model	NRSur PHM	Phenom PHM	SEOBNR PHM
Primary BH mass $m_1 (M_\odot)$	85^{+21}_{-14}	90^{+23}_{-16}	99^{+42}_{-19}
Secondary BH mass $m_2 (M_\odot)$	66^{+17}_{-18}	65^{+16}_{-15}	71^{+21}_{-28}
Total BBH mass $M (M_\odot)$	150^{+29}_{-17}	154^{+25}_{-16}	170^{+36}_{-23}
Binary chirp mass $\mathcal{M} (M_\odot)$	64^{+13}_{-11}	65^{+13}_{-10}	71^{+15}_{-10}
Mass ratio $q = m_2/m_1$	$0.79^{+0.19}_{-0.29}$	$0.73^{+0.24}_{-0.29}$	$0.74^{+0.23}_{-0.42}$
Primary BH spin χ_1	$0.69^{+0.27}_{-0.62}$	$0.65^{+0.37}_{-0.57}$	$0.80^{+0.18}_{-0.58}$
Secondary BH spin χ_2	$0.73^{+0.24}_{-0.64}$	$0.53^{+0.42}_{-0.48}$	$0.54^{+0.41}_{-0.48}$
Primary BH spin tilt angle θ_{LS1} (deg)	81^{+64}_{-49}	81^{+64}_{-45}	81^{+49}_{-45}
Secondary BH spin tilt angle θ_{LS2} (deg)	85^{+57}_{-51}	87^{+53}_{-58}	93^{+51}_{-60}
Effective inspiral spin parameter χ_{eff}	$0.08^{+0.27}_{-0.36}$	$0.05^{+0.31}_{-0.39}$	$0.06^{+0.34}_{-0.35}$
Effective precession spin parameter χ_p	$0.68^{+0.25}_{-0.37}$	$0.60^{+0.33}_{-0.44}$	$0.74^{+0.21}_{-0.40}$
Remnant BH mass $M_f (M_\odot)$	142^{+28}_{-16}	147^{+23}_{-11}	162^{+35}_{-22}
Remnant BH spin χ_f	$0.72^{+0.09}_{-0.12}$	$0.72^{+0.11}_{-0.12}$	$0.74^{+0.12}_{-0.14}$
Radiated energy $E_{\text{rad}} (M_\odot c^2)$	$7.2^{+2.2}_{-1.5}$	$7.2^{+2.2}_{-1.5}$	$7.8^{+2.8}_{-2.8}$
Peak Luminosity $\ell_{\text{peak}} (\text{erg s}^{-1})$	$3.7^{+0.7}_{-0.9} \times 10^{56}$	$3.5^{+0.8}_{-1.1} \times 10^{56}$	$3.5^{+0.8}_{-1.4} \times 10^{56}$
Luminosity distance D_L (Gpc)	$5.3^{+2.4}_{-1.6}$	$4.6^{+1.6}_{-1.8}$	$4.0^{+2.0}_{-1.8}$
Source redshift z	$0.83^{+0.28}_{-0.34}$	$0.73^{+0.20}_{-0.22}$	$0.64^{+0.25}_{-0.26}$
Sky localization $\Delta\Omega$ (deg ²)	774	862	1069





Summary

- We started to filling gaps in stellar graveyard
- First observation of intermediate black hole 100-100 M_{sun}
- First observation of objects from massgap (3-5 M_{sun})
- What's more there were 39 detections of GW in O3a
- We can start population studies